ISBN: 978-3-95450-241-7 ISSN: 2673-5350 doi:10.18429/JACoW-IBIC2022-TUP17

HL-LHC BEAM GAS FLUORESCENCE STUDIES FOR TRANSVERSE PROFILE MEASUREMENT

O. Sedlacek *[1][2], O. Stringer[2], C. Welsch[2], H. Zhang[2]
University of Liverpool, Liverpool, UK
M. Ady, A. R. Churchman, S. Mazzoni, M. Sameed, G. Schneider,
C. C. Sequeiro, K. Sidorowski, R. Veness, CERN, Geneva, Switzerland
P. Forck, S. Udrea, GSI, Darmstadt, Germany
[1]also at CERN, Geneva, Switzerland
[2]also at Cockcroft Institute, Daresbury, Warrington, UK

Abstract

In a gas jet monitor, a supersonic gas curtain is injected into the beam pipe and interacts with the charged particle beam. The monitor exploits fluorescence induced by beam-gas interactions, thus providing a minimally invasive transverse profile measurement. Such a monitor is being developed as part of the High Luminosity LHC upgrade at CERN. As a preliminary study, the fluorescence cross section of relevant gases must be measured for protons at 450 GeV and 6.8 TeV (i.e. the LHC injection and flat top energies). In these measurements, neon, or alternatively nitrogen gas, will be injected into the LHC vacuum pipe by a regulated gas valve to create an extended pressure bump. This work presents the optical detection system that was installed in 2022 in the LHC to measure luminescence cross-section and horizontal beam profile. Preliminary measurements of background light and first signals are presented in this paper.

INTRODUCTION

During the Long Shutdown 3 (LS3, from 2026 to 2028) the Large Hadron Collider (LHC) will undergo a major upgrade to deliver higher luminosity [1], which will involve many new technologies including novel beam diagnostics. A gas jet monitor - Beam Gas Curtain (BGC) monitor - exploiting fluorescence is well-suited for such an environment as it provides non-invasive or minimally invasive profile measurements in the presence of high HL-LHC beam power and strong magnetic fields. The monitor [2–7] is based on a supersonic gas curtain propagating into the path of the beams at 45° that would allow an observation of the 2D transverse distributions from above. The beam excites the gas atoms through collisions which, after deexcitation, emit photons. The distribution of photons is then directly related to the distribution of the original beam. To optimize the detector it is important to know the light yield of the fluorescence process with working gases, such as neon and nitrogen, and protons at 6.8 TeV. Currently, the cross-sections at such high energies are extrapolated through many orders of magnitude from information found in literature at much lower energies [8]. To address this lack of data, an experiment was carried out in 2018 in the LHC to measure neon fluorescence yield at the LHC beam energies, but due to a high background and a low cross-section, only the fluorescence caused by heavy lead ions at the injection energy was measured. Therefore, a new experimental setup was installed at the LHC with many improvements implemented in order to reduce synchrotron radiation background and to improve the sensitivity. The experimental setup is described in this paper, together with the first measurements performed during beam operation in 2022.

EXPERIMENTAL SETUP

A new imaging system was designed and installed at the LHC point 4 on the ‘Beam 1’ line (i.e. beam propagating clockwise) in a vacuum chamber equipped with a gas injection system with the aim of measuring the LHC beam-induced fluorescence yield of neon at 585 nm. Neon gas is injected at a pressure of 5×10^{-8} mbar to minimise its effect on the beam quality while providing enough gas atoms for the beam to collide with. The observed process is an emission line of neutral Ne which is due to the $2s^2 2p^5 (^2P^0_{1/2}) 3p^2 [1/2]_0 \rightarrow 3s^2[1/2]_1$ transition at 585.4 nm [2,9].

Figure 1 depicts the whole experimental setup including the camera module which measures the distribution of the emitted photons. An optical line is installed on top of a window flange, imaging the photons with an apochromatic triplet lens with an aperture of 40 mm and a focal length of 160 mm ideal for near-1:1 imaging conditions. The lens provides a high transmittance of approximately 80 % over the wavelengths of interest. In front of the sensor, a filter wheel is installed with one empty filter socket, one blocking filter and one 585 ± 10 nm filter. The blocking filter is a completely opaque screen stopping any photons from reaching the sensor and is used for background studies. The 585 ± 10 nm filter then allows the fluorescence signal to be measured while reducing other sources of background light. The fluorescence light is measured by a two-stage image intensifier reaching single-photon detection sensitivity [10].

The experimental chamber was installed during the 2021-22 LHC Year-End Technical Stop (YETS), in a position where low levels of synchrotron radiation are expected. To minimise the reflection of synchrotron radiation, the vacuum chamber was also blackened by amorphous carbon coating with a reflectivity of 14 %. An ultra-low reflectivity black

---

* Ondrej.Sedlacek@cern.ch

contrast plate with multi-layered coating with a reflectivity of 0.25 % was also installed at the bottom of the chamber on the opposite side of the vacuum window to minimise background light reaching the camera.

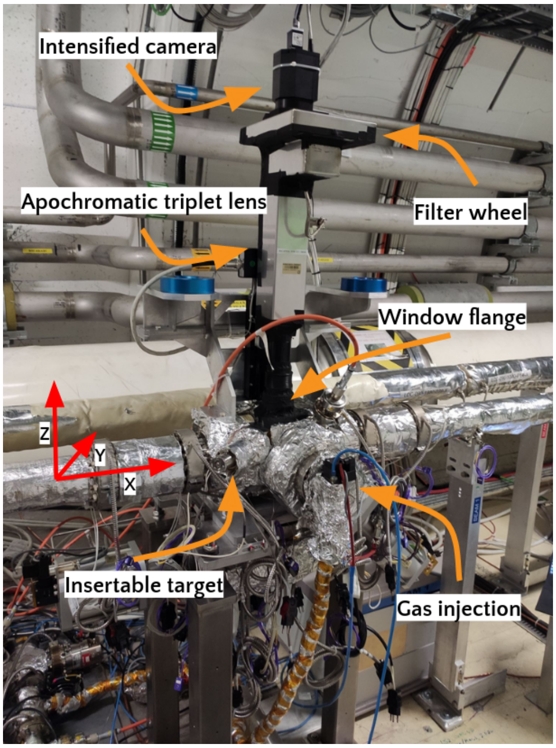

Figure 1: The experimental setup installation in the LHC, consisting of a blackened chamber, a gas injection system and a camera module.

OPTICAL SYSTEM

The extrapolated cross-section of the fluorescence is 4.7×10^{-22} cm^2 [8]. In order to cope with such a low light yield, the optical system was designed to demagnify the final image and increase the number of photons per pixel, while keeping the resolution small enough to measure the LHC beam size and maintaining the optical acceptance as large as possible. The final trade-off magnification of the system is set to 0.205 with 10.5 pixels per 300 µm corresponding to the LHC beam σ. Therefore, the solid angle of the system is 1.8×10^{-2} sr and its acceptance is 1.4×10^{-3}.

The Modulation Transfer Function (MTF) of the optical module was measured to evaluate the optical performance of the system. The resulting MTF is summarized in Table 1 which shows that for the expected beam size of 1.2 mm (4σ) the MTF is >46 % and in the order of 300 µm (σ) the MTF is still >26 %. The measurements were carried out at 585 nm using a movable optical target.

LHC BACKGROUND MEASUREMENTS

Background measurements in presence of the LHC beam at 6.8 TeV without injecting gas are shown in Figs. 2-4 and discussed below. In the figures, the beam propagates along the X-axis from left to right. The Y-axis corresponds to the horizontal direction transverse to the beam's trajectory as labeled in Fig. 1. With no gas injection in these measurements, the signal observed on the camera corresponds to the background signals caused by different sources.

Table 1: Measured Modulation Transfer Function (MTF) of the optical module installed at LHC showing MTF >46 % for 1.2 mm corresponding to 4σ of the LHC beam.

MTF [%]	**line/mm**
46	1.000
38	0.500
26	0.250
13	0.125

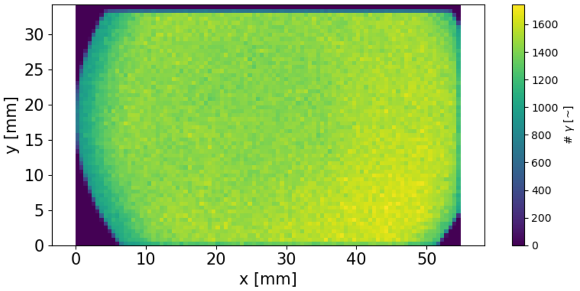

Figure 2: Background measurement in presence of the LHC beam at 6.8 TeV with a blocking filter. The measured signal yield corresponds to the beam loss induced photon-like signal as measured by the camera.

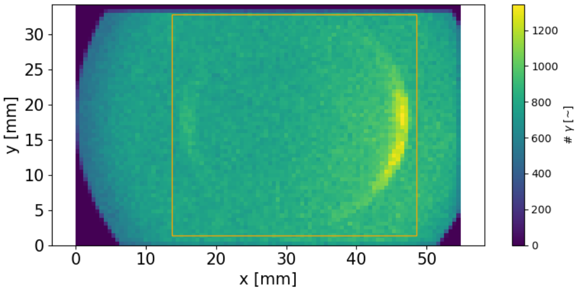

Figure 3: Measurement of the LHC beam at 6.8 TeV with a 585 ± 10 nm filter corresponding to the distribution of beam loss induced signal and synchrotron radiation observed by the camera module.

The dark counts from the camera and the optical light background measured without beam were found to be negligible. The natural beam losses at those locations typically come from the interaction of the beam with rest-gas molecules. They generate particle showers that can induce photon-like signals while crossing the MCP. The beam loss (and negligible dark counts) signal was measured using the blocking plate in the optical filter wheel such that no photon would reach the camera. Figure 2 shows that in such a case the

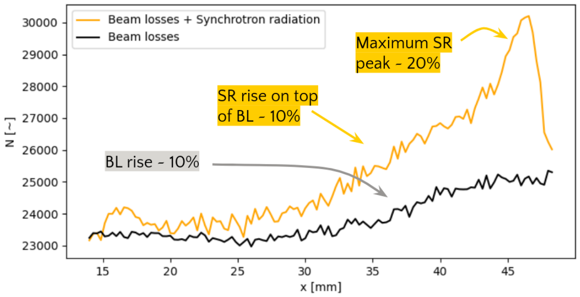

Figure 4: X projection (sum across y) of measurements with the 585 ± 10 nm (orange line) and Blocking (black line) filter.

distribution of losses is not perfectly homogeneous. A horizontal projection of the image, depicted in Fig. 4, clearly demonstrates that the photon distribution is not perfectly homogeneous which is not fully understood at this stage.

The synchrotron radiation background at the 585 nm wavelength was then measured by replacing the blocking filter with the 585 nm optical band-pass filter. The corresponding image is shown in Fig. 3. It clearly shows that, at the top energy, synchrotron radiation, generated in the surrounding dipole magnets, is the main source of optical light background for this measurement. As shown in Fig. 4, the distribution of synchrotron radiation presents an even larger inhomogeneity.

Integrating over all pixels of the image in Fig. 3, the synchrotron radiation accounts for only 3.7 % of all observed signals. Additionally, if we consider only the area around the window flange (e.g area of the image that is looking inside of the tbeam pipe), depicted as the orange rectangle in Fig. 3, then the synchrotron radiation makes up about 6 % of all signals.

Overall the synchrotron radiation levels are quite low, especially in comparison to the previous measurements carried out in 2018. The tests performed at a different location in the LHC and using a different setup demonstrated that synchrotron radiation accounted for 30 % of the signal. The measurements done in 2018 had also much higher beam loss signals, therefore it is difficult to quantify by how much the synchrotron radiation background has been reduced. Nonetheless, this is a very valuable improvement which can be attributed to the new vacuum chamber with blackened, light-absorptive internal surfaces.

SIGNAL VS BACKGROUND

With the presented experimental setup and the current settings, the expected level of fluorescence signal should be visible above the background if using a sufficient integration time. In the present configuration, the fluorescence signal should appear as a continuous horizontal band in the image. Due to the inhomogeneity of the background, the fluorescence signal should appear more clearly in the central part of the images as shown in Fig. 5 by the orange box.

The results presented in Figs. 5 and 6, show a small fluorescence signal at the expected position. This first, but very encouraging, measurement was carried out with a gas pressure at the interaction point in the order of 2×10^{-8}mbar, and with ~ 2000 nominal bunches at 6.8 TeV. The measurement's integration time was 450 s.

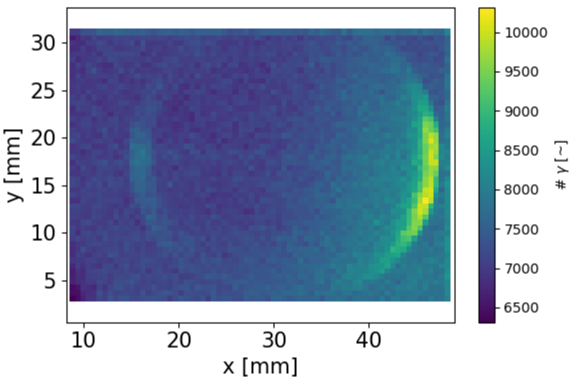

Figure 5: Image acquired using the 585 ± 10 nm filter.

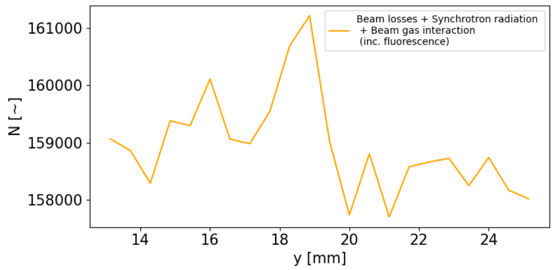

Figure 6: Vertical projection of image depicted in Fig. 5.

CONCLUSIONS

New imaging and gas injection systems were installed in the LHC to measure the neon fluorescence light yield with protons at 6.8 TeV. A first set of measurements showed that beam loss and synchrotron radiation signals dominate the background with synchrotron radiation accounting for 6 % of all observed signals in the central area of the image and beam losses to the remaining 94 %. In those conditions, a small fluorescence signal was observed for the very first time with protons at 6.8 TeV using a long integration time. More measurements will be performed in the coming months as the LHC intensity ramp up continues. In the next phase of our work, we will concentrate on neon fluorescence cross section at the injection and top energies with both protons and heavy ions. In the coming year, the gas injection system will be replaced with a supersonic gas curtain that would enable the local gas density to be increased by two orders of magnitude. This will result in more precise measurements of the fluorescence cross section and non-invasive beam profile measurements.

ACKNOWLEDGMENTS

This work was supported by STFC under grant agreement ST/P006752/1 and is a part of HL-LHC project.

REFERENCES

[1] G. Apollinari *et al.*, “High luminosity large hadron collider HL-LHC”, 2017. `doi:10.48550/arXiv.1705.08830`

[2] S. Udrea *et al.*, “Development of a Fluorescence Based Gas Sheet Profile Monitor for Use With Electron Lenses: Optical System Design and Preparatory Experiments”, in *Proc. 6th Int. Beam Instrumentation Conf. (IBIC’17)*, Grand Rapids, MI, USA, Aug. 2017, pp. 359–363. `doi:10.18429/JACoW-IBIC2017-WEPCC08`

[3] A. Salehilashkajani *et al.*, “Commissioning of the Prototype for a New Gas Curtain Beam Profile Monitor Using Beam Induced Fluorescence for HL-LHC”, in *Proc. 10th Int. Particle Accelerator Conf. (IPAC’19)*, Melbourne, Australia, May 2019, pp. 2709–2712. `doi:10.18429/JACoW-IPAC2019-WEPGW093`

[4] V. Tzoganis and C. P. Welsch. “A non-invasive beam profile monitor for charged particle beams”, *Appl. Phys. Lett.*, vol. 104, no. 20, p. 204104, 2014. `doi:10.1063/1.4879285`

[5] H. D. Zhang *et al.*, “A Supersonic Gas-Jet Based Beam Induced Fluorescence Prototype Monitor for Transverse Profile Determination”, in *Proc. 8th Int. Particle Accelerator Conf. (IPAC’17)*, Copenhagen, Denmark, May 2017, pp. 458–461. `doi:10.18429/JACoW-IPAC2017-MOPAB139`

[6] H. D. Zhang *et al.*, “A Supersonic Gas Jet-Based Beam Profile Monitor Using Fluorescence for HL-LHC”, in *Proc. 9th Int. Particle Accelerator Conf. (IPAC’18)*, Vancouver, Canada, Apr.-May 2018, pp. 1891–1894. `doi:10.18429/JACoW-IPAC2018-WEPAF034`

[7] A. Salehilashkajani *et al.*, “A gas curtain beam profile monitor using beam induced fluorescence for high intensity charged particle beams”, *Appl. Phys. Lett.*, vol. 120, no. 17, p. 174101, 2022. `doi:10.1063/5.0085491`

[8] S.Udrea and P. Forck, “Milestone 1.6 report”, GSI, Darmstadt, Germany, 2018.

[9] M. Eckhardt, D. Hasselkamp, and K.H. Schartner, “Neon 3p-excitation by proton impact (100 keV-1 MeV): Cross sections and line polarization”, *Z Physik A*, Dec. 1979, vol. 292, pp. 337–345. `doi:10.1007/BF01546431`

[10] S. Udrea *et al.*, “Development of a fluorescence based gas sheet profile monitor for use with electron lenses: Optical System design and preparatory experiments”, in *Proc. 6th Int. Beam Instrumentation Conf. (IBIC’17)* Grand Rapids, MI, USA, Aug. 2017. `doi:10.18429/JACoW-IBIC2017-WEPCC08`